New Phytologist

Research

PROGRAMMED CELL DEATH8 interacts with tetrapyrrole biosynthesis enzymes and ClpC1 to maintain homeostasis of tetrapyrrole metabolites in Arabidopsis

Rudan Geng[1], Xiaoqing Pang[2], Xia Li[1], Shanshan Shi[1], Boris Hedtke[2], Bernhard Grimm[2], Ralph Bock[3], Jirong Huang[4] and Wenbin Zhou[1]

[1]Institute of Crop Sciences, Chinese Academy of Agricultural Sciences, Beijing 100081, China; [2]Institute of Biology/Plant Physiology, Humboldt-Universität zu Berlin, Philippstraße 13, Berlin 10115, Germany; [3]Max-Planck-Institut für Molekulare Pflanzenphysiologie, Am Mühlenberg 1, D-14476 Potsdam-Golm, Germany; [4]Shanghai Key Laboratory of Plant Molecular Sciences, College of Life Sciences, Shanghai Normal University, Shanghai 200234, China

Author for correspondence:
Wenbin Zhou
Email: zhouwenbin@caas.cn

Received: *2 January 2023*
Accepted: *19 March 2023*

New Phytologist (2023) **238:** 2545–2560
doi: 10.1111/nph.18906

Key words: Clp protease, PCD8, programmed cell death, singlet oxygen, tetrapyrrole biosynthesis.

Summary

- Tetrapyrrole biosynthesis (TBS) is a dynamically and strictly regulated process. Disruptions in tetrapyrrole metabolism influence many aspects of plant physiology, including photosynthesis, programmed cell death (PCD), and retrograde signaling, thus affecting plant growth and development at multiple levels. However, the genetic and molecular basis of TBS is not fully understood.
- We report here PCD8, a newly identified thylakoid-localized protein encoded by an essential gene in *Arabidopsis*. *PCD8* knockdown causes a necrotic phenotype due to excessive chloroplast damage. A burst of singlet oxygen that results from overaccumulated tetrapyrrole intermediates upon illumination is suggested to be responsible for cell death in the knockdown mutants.
- Genetic and biochemical analyses revealed that PCD8 interacts with ClpC1 and a number of TBS enzymes, such as HEMC, CHLD, and PORC of TBS.
- Taken together, our findings uncover the function of chloroplast-localized PCD8 and provide a new perspective to elucidate molecular mechanism of how TBS is finely regulated in plants.

Introduction

Chloroplasts not only perform the essential process of photosynthesis, but also are the site to biosynthesize a large variety of important compounds such as tetrapyrroles, vitamins, amino acids, fatty acids, and phytohormones (Neuhaus & Emes, 2000). Besides their basic function as a major hub of plant metabolism, chloroplasts have been demonstrated to be sensors for environmental changes and play a pivotal role in the regulation of plant growth and development (Jarvis & Lopez-Juez, 2013). The tetrapyrrole biosynthesis (TBS) pathway consists of > 20 highly regulated enzymatic steps and starts from 5-aminolevulinic acid (ALA), followed by porphyrin synthesis, until protoporphyrin IX (Proto IX) is chelated with ferrous ions and Mg^{2+} cations in heme and chlorophyll biosynthesis, respectively (Wang & Grimm, 2021). Chlorophyll biosynthesis is a prerequisite for light-dependent chloroplast biogenesis and is tightly controlled in response to developmental programs and environmental cues (Neuhaus & Emes, 2000; Inaba & Ito-Inaba, 2010; Jarvis & Lopez-Juez, 2013). Impaired chlorophyll biosynthesis or catabolism will generate higher levels of reactive oxygen species (ROS) due to accumulation of highly photoreactive molecules, such as free chlorophyll and its intermediates (De Pinto *et al.*, 2012; Wang & Bayles, 2013).

Chlorophylls, chlorin, and porphyrin intermediates are potential photosensitizers that can transfer excitation energy to $^3O_2$, leading to production of singlet oxygen ($^1O_2$) (Demmig-Adams & Adams, 2000; Meskauskiene *et al.*, 2001; Woodson *et al.*, 2015). The conditional *fluorescent* (*flu*) mutant of *Arabidopsis* overaccumulates free protochlorophyllide (Pchlide) and generates excessive amounts of $^1O_2$ after transfer from dark to light, thus leading to cell death (Meskauskiene *et al.*, 2001; Laloi *et al.*, 2007; Kim *et al.*, 2009). Interestingly, the cell death phenotype of *flu* is not directly caused by the toxicity of $^1O_2$, but requires the proteins EXECUTER1 and EXECUTER2 (EX1/2) (Lee *et al.*, 2007; Kim *et al.*, 2012). It has been shown that these proteins are necessary for the initiation of $^1O_2$-derived retrograde signaling (Dogra *et al.*, 2019, 2022) and function as transducers or sensors for $^1O_2$-induced gene expression and the stress-related cell death response (Lee *et al.*, 2007). The *Arabidopsis* conditional *lesion simulating disease1* (*lsd1*) mutant, defective in proper protein assembly of photosynthetic complexes due to uncoupled

expression of nuclear and plastid photosynthesis-associated genes, also produces excessive amounts of $^1O_2$ resulting in day-length-dependent cell death, which is dependent on EX1 (Lv *et al.*, 2019). Recently, the *Arabidopsis* conditional *ferrochelatase 2* (*fc2*) mutant was reported to accumulate excess protoporphyrin IX (Proto IX) and consequently suffered from severe photooxidative damage of chloroplasts upon exposure to light (Woodson *et al.*, 2015). Genetic screening for suppressor mutants revealed that the envelope membrane proteins in disrupted chloroplasts in *fc2* are ubiquitinated through the Plant U-Box 4 (PUB4)-mediated ubiquitin-dependent quality control pathway. However, unlike *flu* and *lsd1*, the phenotype of *fc2* mutants cannot be suppressed by the *ex1* mutations (Woodson *et al.*, 2015).

Another $^1O_2$ signaling pathway independent of EX1 has also been reported. The *chlorina 1* (*ch1*) mutant is defective in chlorophyll *a* oxygenase, resulting in the absence of chlorophyll *b*. The cell death phenotype of the *ch1* mutant is caused by overaccumulation of $^1O_2$ due to overexcitation of PSII reaction centers under excess light. $^1O_2$-induced cell death in *ch1* is dependent on the OXIDATIVE STRESS INDUCIBLE 1 protein (Shumbe *et al.*, 2016). The $^1O_2$ signal can be transmitted through the carotenoid degradation products β-cyclocitral (β-cc) and dihydroactinidiolide to modulate nuclear gene expression and detoxification pathways (D'Alessandro *et al.*, 2018, 2020). Interestingly, genetic screening for suppressor mutants of the *flu ex1* double mutant identified a new $^1O_2$-induced EX1-independent retrograde signaling pathway (Wang *et al.*, 2020). Disruption of the gene encoding the stroma-localized chloroplast protein $^1O_2$-SAFEGUARD1 (SAFE1) upon illumination leads to accumulation of Pchlide and overproduction of $^1O_2$ in the grana margin of the thylakoids, and ultimately to cell death. These studies suggest that distinctive $^1O_2$ signaling pathways exist in different subcompartments of the chloroplast. However, molecular mechanisms by which $^1O_2$ initiates different signals and their signaling pathways in the chloroplast remain unknown.

Programmed cell death (PCD) is a fundamental and genetically controlled process that has important functions in plant development and responses to biotic and abiotic stresses (Pennell & Lamb, 1997; Huysmans *et al.*, 2017). Increasing evidence supports that ROS produced in chloroplasts play a central role in PCD of green tissues (Van Aken & Van Breusegem, 2015). Consistently, functional chloroplasts and light are required to trigger PCD in plants (Kim *et al.*, 2012). For example, mutants that are defective in genes involved in chlorophyll biosynthesis including *coproporphyrinogen oxidase* (*cpo*), *uroporphyrinogen decarboxylase* (*urod*), *rugosa1* (*rug1*), *fc2*, and *flu* display necrotic phenotypes (Kruse *et al.*, 1995; Mock & Grimm, 1997; Hu *et al.*, 1998; Mock *et al.*, 1999; Ishikawa *et al.*, 2001; Meskauskiene *et al.*, 2001; Ayliffe *et al.*, 2009; Huang *et al.*, 2009; Quesada *et al.*, 2013; Woodson *et al.*, 2015). These mutants accumulate photoreactive chlorophyll intermediates and generate ROS upon illumination. Considerable progress has been made toward our understanding of the control and execution of PCD via identification of suppressors for necrotic or lesion-mimic mutants. Thus, searching for more players in PCD will provide new entry points to dissect the complex molecular basis of PCD.

In this study, we identified an unknown thylakoid-localized protein, PCD8, which is required for homeostasis of TBS, and interacts with Clp protease and TBS proteins. Our data suggest that PCD8 may control proteolysis of TBS proteins by directing the Clp protease to these enzymes.

Materials and Methods

Plant materials and growth conditions

The *Arabidopsis thaliana* ecotype Columbia (Col-0) was used as wild-type (WT). T-DNA insertion lines were obtained from the European *Arabidopsis* Stock Centre (NASC): *pcd8-1* (SALK_006849), *pcd8-2* (SALK_087872), and *clpC1* (SALK_014058). The *ex1*, *gun4*, and *gun5* mutants were reported previously (Supporting Information Table S1) and kindly gifted by Professors Klaus Apel and Chanhong Kim, Joanne Chory and Jesse D. Woodson, and Robert Larkin, respectively. Double mutants were obtained by crossing mutant lines, and all genotypes were confirmed by PCR-based analyses.

Seeds were surface-sterilized in 2% hypochlorite solution for 15 min and washed three times with sterile water. Seeds were then plated on half-strength MS medium containing 0.7% (w/v) agar. After stratification at 4°C in darkness for 3 d, seeds were placed in a growth chamber under 24 h light (CL), 16 h : 8 h, light : dark (LD), or 8 h : 16 h, light : dark (SD) conditions. The light intensity was maintained at 120 μmol photons m^{-2} s^{-1} at 22°C. For excess light treatment experiments, 4-wk-old seedlings were incubated in 8 h : 16 h, light : dark for 6 d at 1000 μmol photons m^{-2} s^{-1}. For dim light experiments, seedlings were grown in 8 h : 16 h, light : dark for 7 wk or 24 h light for 6 wk at 20 μmol photons m^{-2} s^{-1}. To obtain etiolated seedlings, plates were wrapped in tin foil for 4 d, and seedlings were harvested under dim green light.

Generation of *PCD8* RNAi plants

The AGRIKOLA collection of RNAi vectors (Hilson *et al.*, 2004) was ordered from NASC, and used to generate a large number of *Arabidopsis* RNAi mutant lines. For the generation of *PCD8* RNAi plants, the vector used to downregulate *Arabidopsis PCD8* was plasmid CATMA2a37310 which carried a 232-bp PCR product corresponding to positions 2532–2763 of the *PCD8* coding region. The gene-specific tags of *PCD8* (in CATMA2a37310) were recombined from the pENTR207 vector into pK7GWIWG2(I). The generated vectors were then transformed into the *Agrobacterium tumefaciens* strain GV3101 and introduced into WT plants via the floral dip method (Clough & Bent, 1998). Transgenic plants were selected for kanamycin resistance by germination of surface-sterilized seeds on agar-solidified half-strength MS medium containing 1% sucrose and 50 mg l^{-1} kanamycin.

Construction of transformation vectors and generation of transgenic plants

To produce a PCD8-GFP fusion vector, the CDS of *PCD8* was amplified from cDNA adding *EcoR*I and *BamH*I restriction sites,

and the PCR products were cloned into the CaMV 35*S*-based pEZR(H)-LN binary vector to generate an in-frame fusion to *GFP* (with GFP at the C-terminus). To express an unfused chloroplast-localized GFP (cpGFP), the *Arabidopsis* RBCS1B transit peptide was amplified and cloned into vector pEZR(H)-LN. To generate cpGFP and PCD8-GFP lines in the *PCD8* RNAi-21 background, the cpGFP and PCD8-GFP transgenic lines produced by transformation of the WT were crossed with the *PCD8* RNAi-21 mutant followed by selection of homozygous lines.

For subcellular localization experiments, the PCD8 cDNA (without the stop codon) was cloned into the Gateway-compatible vector pENTR-D/TOPO (Invitrogen) and then transferred to the CaMV 35*S*-based vector pGWB5 with the GFP at the C-terminus using LR clonase (Invitrogen). For complementation experiments, to express PCD8 from its native promoter and 3′ UTR, the promoter-less vector pGWB4 was used instead. Both vectors confer kanamycin and hygromycin resistance to plants. The generated vectors were transformed into *A. tumefaciens* strain GV3101. Transgenic *Arabidopsis* plants were generated using the floral dip procedure (Clough & Bent, 1998).

Co-immunoprecipitation and mass spectrometric protein identification

The μMACS GFP-tagged protein isolation kit (Miltenyi Biotec, Bergisch Gladbach, Germany) was used to isolate protein complexes from plants expressing the PCD8-GFP fusion protein. Proteins that bind nonspecifically to the anti-GFP antibody beads were excluded by using WT and cpGFP seedlings as negative controls. Total cellular protein was extracted from 10 g fresh seedlings from three plant lines (PCD8-GFP, WT, and cpGFP) on ice in lysis buffer (20 mM Tris, pH 7.5, 150 mM NaCl, 1 mM EDTA, 0.5% (v/v) Triton X-100, 5 μg ml^{-1} aprotinin, and protease inhibitor cocktail from Roche). After centrifugation at 4°C for 15 min, the supernatants were mixed with 100 μl of anti-GFP microbeads (Miltenyi Biotec) and incubated on ice for 30 min with shaking. To capture the magnetic antigen–antibody complex, the mixtures were applied to μColumns (Miltenyi Biotec) in a magnetic field. Lysis buffer was used to wash the samples on the column, and immunoprecipitants were eluted with 100 μl of elution buffer. After immunoprecipitation, the eluted proteins were separated in SDS-PAGE and stained with Coomassie Brilliant Blue. Subsequently, each lane was cut into several gel slices. In-gel tryptic digestion and mass spectrometry were performed as described previously (Albus *et al.*, 2010). The spectra obtained from tandem mass spectrometry were evaluated against the TAIR10 database using Mascot (Matrix Science, Boston, MA, USA). Proteins identified by mass spectrometry were filtered by the following criteria: identification in the PCD8-GFP sample, but not in the cpGFP sample; and protein localized in chloroplasts according to published information or as predicted by TargetP (http://www.cbs.dtu.dk/services/TargetP/). Putative interaction partners of PCD8 identified are listed in Table S2.

BiFC assays

Bimolecular fluorescence complementation (BiFC) assays were performed using a split-YFP system in *Arabidopsis* protoplast. Briefly, the coding sequence of *PCD8*, *ClpC1*, *HEMC*, *PORC*, *CHLD*, *HSP21*, and *pTAC5* were cloned into pUC-SPYNE and pUC-SPYCE (Zhong *et al.*, 2013), and plasmids were cotransformed into *Arabidopsis* protoplasts isolated from WT as described previously (Yoo *et al.*, 2007). Protoplasts were then incubated in dark for 12–16 h, and fluorescence signals were observed with a confocal microscope (Zeiss LSM700). Primers are listed in Table S3.

HPLC measurements of uroporphyrinogen I and III and other tetrapyrrole intermediates

The levels of the five tetrapyrrole intermediates uroporphyrinogen I and III (Uro I and Uro III), coproporphyrinogen III (Copro III), protoporphyrin IX (Proto IX), and Mg-Protoporphyrin IX (MgP) were measured by HPLC analysis as described previously (Czarnecki & Grimm, 2012). Briefly, plants were grown under SD for 3 wk, rosette leaves (*c.* 100 mg) were harvested, their fresh weight (FW) were determined, and the materials were ground in liquid nitrogen. Tetrapyrroles were extracted with 500 μl 50 mM potassium phosphate buffer (pH 7.8) and centrifuged at 10 000 ***g*** (at 4°C for 10 min). The supernatant was collected, the pellet was washed with 500 μl 10% (v/v) 0.1 M NH_4OH and 90% (v/v) methanol and centrifuged at 10 000 ***g*** for 10 min at 4°C. The supernatants were then combined, and the pellet re-extracted with 500 μl 10% (v/v) 0.1 M NH_4OH and 90% (v/v) methanol by vortexing for 2 min, followed by incubation at −20°C for 20 min, and centrifugation at 16 000 ***g*** at 4°C for 10 min. All extracts were then combined and centrifuged at 16 000 ***g*** at 4°C for 10 min, the supernatant was collected, passed through a 0.22 μm mesh filter, and a sample of 400 μl was transferred to a brown vial. For quantification of Uro III, Copro III, and Proto IX, 10 μl of 1 M acetic acid and 10 μl of 2-butanone were added before injection into the HPLC. Tetrapyrroles were separated on an Agilent X-bridge C_{18} column (5 μm, 250 mm × 4.6 mm) with the following HPLC method: solvent A: methanol; solvent B: 0.1 mM ammonium acetate (pH 5.2); flow rate: 1.0 ml min^{-1}; column temperature: 25°C. The elution of tetrapyrroles was monitored by fluorescence (2695; Waters, Milford, MA, USA). For detection of Uro III, Copro III, and Proto IX, E_x/E_m 405/625 nm was used, for detection of MgP, E_x/E_m 420/595 nm. Authentic tetrapyrroles (Frontier Scientific, Newark, DE, USA) were used as standards to calculate calibration curves and determine elution times.

Pull-down assays

The coding sequences of *PCD8*, *HEMC*, *PORC*, and *ClpC1* (without transit peptide) were inserted into the pGEX-4 T-1, pET-32a, or pCZN1 vectors to generate fusion proteins with GST or Trx + His_6 or His_6, respectively. The vectors were transformed into *Escherichia coli* strain Top10 and induced with

0.5 mM IPTG at 16°C for 20 h. The culture was then sonicated, and the supernatant collected. Using a low-pressure chromatography system, the supernatant was loaded onto a Ni-IDA-Sepharose Cl-6B affinity chromatography column at a flow rate of 0.5 ml min^{-1}. The collected protein solution was transferred to a dialysis bag and dialyzed against PBS overnight, before 12% SDS-PAGE analysis. Pull-down assays were performed according to a published protocol (Miernyk & Thelen, 2008), and proteins were detected with anti-GST or anti-His antibodies used at 1 : 1000 dilution.

Electron microscopy

Transmission electron microscopy (TEM) analyses were performed as described previously (Izumi *et al.*, 2017). Seedlings were grown in the dark for 4 d and transferred to the light for 12 h. Seedlings were removed from plates and immediately immersed in a solution of 2.5% glutaraldehyde and vacuum-infiltrated. Seedling cotyledons were observed and imaged on a TEM at 120 kV (HT7700; Hitachi, Ibaraki, Japan).

Pigments measurements

For measurements of pigment contents, seedlings were harvested and, after measurement of their fresh weight, frozen in liquid nitrogen and homogenized. Chlorophyll and total carotenoids were extracted in 1 ml ice-cold 100% acetone, and cell debris was removed by centrifugation at 5000 ***g*** for 15 min at 4°C. Absorption was measured at 661.6, 644.8, and 470 nm (Lichtenthaler, 1987). Anthocyanin was extracted in 450 µl methanol: HCl (99 : 1). Subsequently, 300 µl deionized water and 750 µl chloroform were added, and the supernatant was collected after centrifugation at 1600 ***g*** for 20 min at 4°C. Absorption was measured at 530 and 657 nm (Rabino & Mancinelli, 1986).

Isolation of chloroplasts, thylakoid membranes, and stroma proteins

All chloroplast isolation procedures were performed at 4°C. Around 50 g leaves (4-wk-old WT plants grown in SD) were homogenized for 2 × 3 s using a Waring blender in 200 ml cold isolation buffer (50 mM HEPES/KOH, pH 8.0, 0.33 M sorbitol, 1 mM $MgCl_2$, 1 mM $MnCl_2$, 2 mM EDTA, 0.1% (w/v) BSA and 0.1% (w/v) isoascorbic acid). The homogenate was filtered through a double layer of Miracloth and then centrifuged at 1500 ***g*** for 2 min, and the pellet was gently resuspended in 12 ml isolation buffer. The suspended chloroplasts were loaded onto a 40/80% v/v two-step Percoll (Sigma) gradient and centrifuged at 2500 ***g*** for 21 min (acceleration set to 1 and deceleration set to 0). The intact chloroplasts appeared in the phase between 40% and 80% Percoll. The intact chloroplasts were recovered, washed with HS buffer (50 mM HEPES/KOH, pH 8.0, 0.33 M sorbitol), and then centrifuged at 700 ***g*** for 5 min. Thylakoid membranes and stroma proteins were prepared from the isolated intact chloroplasts according to pervious report (Salvi *et al.*, 2008).

Results

PCD8 RNAi mutants display necrotic spots during dark-to-light transition

To identify new regulatory components involved in the plant PCD, we screened: *Arabidopsis* mutants for necrotic phenotypes using a collection of T-DNA insertion lines obtained from the Nottingham *Arabidopsis* Stock Centre; and RNA interference (RNAi) mutants that we produced with the AGRIKOLA collection of RNAi vectors (http://www.arabidopsis.info/). A number of *pcd* mutants that exhibited necrotic lesions after transition from dark to light or under short-day (SD; 8 h : 16 h, light : dark cycles) vs long-day (LD, 8 h : 16 h, light : dark cycles) conditions were identified. Interestingly, one of the *pcd* mutants, designated *pcd8*, was found to display extensive necrotic spots under short-day conditions. The *pcd8* phenotype was produced by an RNAi approach due to knockdown expression of the gene locus At2g39080. We selected three representative RNAi lines (RNAi-6, RNAi-14, and RNAi-21) for subsequent in-depth analysis. Some necrotic lesions and a slight growth retardation were also observed in these LD-grown *PCD8* RNAi lines (Fig. 1a). However, the phenotypes were more severe when the mutant plants were grown under SD (Fig. 1b). Interestingly, no necrotic leaf spots were found in leaves of RNAi lines grown under continuous light conditions (CL; 24 h of light; Fig. 1c), indicating that the regular dark-to-light transition is an important environmental factor to cause the necrotic phenotype of *pcd8*. To exclude the possibility that excess light causes the photooxidative damage, WT, and *pcd8* plants were grown under SD and CL conditions with a low light intensity of 30 µmol photons m^{-2} s^{-1}. The mutants showed necrotic lesions in SD but not in CL condition (Fig. S1a,b). Taken together, our data suggest that the visible necrotic lesions in *pcd8* leaves are tightly associated with the change to darkness during photoperiodic growth.

Consistent with the severity of the phenotypes, quantitative PCR (qPCR) analysis showed that the *PCD8* transcript level was the lowest in the line RNAi-21 (3% of WT *PCD8* expression; Fig. 1d), followed by the line RNAi-14 (5%) and the line RNAi-6 (80%). To assess protein levels in the RNAi knockdown lines, a specific polyclonal antibody against PCD8 was produced. Immunoblot analysis demonstrated that the levels of PCD8 were dramatically reduced in RNAi-14 and RNAi-21 plants but modestly in RNAi-6 plants (Fig. 1e). Taken together, our results suggest that PCD8 is a new important factor preventing PCD during photoperiodic growth.

PCD8 predominantly localizes to thylakoids and is essential for plant survival

To further confirm that silencing of *PCD8* expression is causally responsible for the cell death phenotype, we searched the collection of publicly available *Arabidopsis* T-DNA insertion lines (http://arabidopsis.info/) for null mutants. Two independent T-DNA insertion lines (SALK_006849 and SALK_087872)

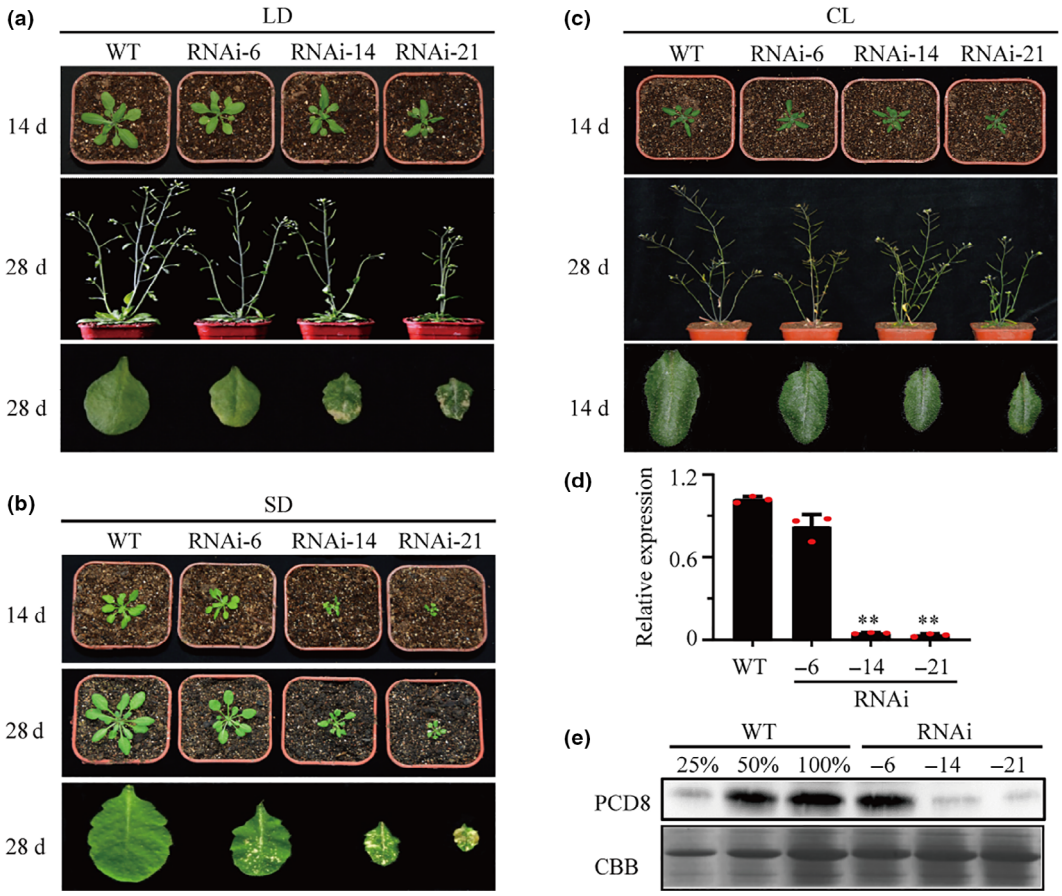

Fig. 1 Arabidopsis *PCD8* RNAi mutants show leaf necrosis during dark-to-light transition. (a–c) Phenotypes of 14- and 28-d-old plants grown under LD (a), SD (b), or CL (c) conditions. LD, long-day (16 h : 8 h, light : dark); SD, short-day (8 h : 16 h, light : dark); CL, continuous light (24 h light). (d) *PCD8* expression level in 28-d-old plants grown in SD. The *EF1α* gene (encoding the alpha-chain of translation elongation factor eEF-1) served as internal control. Data are means ± standard deviation, $n = 3$ biological repetitions. Student's *t*-test: **, $P < 0.01$. (e) PCD8 protein levels in 28-d-old plants grown under SD conditions. The denaturing polyacrylic acid gel stained with Coomassie Brilliant Blue (CBB) is shown below the immunoblot as a control for equal loading.

associated with the *PCD8* locus (At2g39080) were available. Both lines contain the T-DNA insertion in the first exon of the *PCD8* gene (Fig. 2a). To obtain homozygous *pcd8* mutants, the mutant lines were self-crossed, and their progenies were genotyped for homozygosity of the T-DNA insertion by PCR (Fig. 2b). Despite genotyping of more than 30 offspring from each line, not a single homozygous plant could be identified, and the ratio of heterozygote to WT was nearly 2 : 1. This finding raises the possibility that *PCD8* inactivation causes embryo lethality. To test this hypothesis, the phenotypes of immature seeds in developing siliques were analyzed. In both mutants, approximately one fourth of the seeds were smaller and less pigmented, suggesting that they contain aborted embryos (Fig. 2c). We also attempted to complement both mutants by expressing the *PCD8* gene under the control of its native promoter in the *pcd8-1* and *pcd8-2* background. The seed phenotype of mutants was rescued in these transgenic complementation lines (Fig. 2d). To directly confirm embryo lethality of *pcd8-1* and *pcd8-2*, embryogenesis was investigated during seed development. Our results showed that development of some embryos from *PCD8/+* siliques was arrested at the heart stage (Fig. 2e). In summary, our results suggest that *PCD8* is an essential gene for plant survival.

As essentiality for embryo survival was the only previously known feature of the *PCD8* gene, it was preliminarily named EMB2799 (for 'embryo-defective'). The putative gene product belongs to the NAD(P) Rossmann-fold superfamily of proteins. Phylogenetic analysis revealed that PCD8 is highly conserved in seed plants and also present in the moss *Physcomitrella patens*, the alga *Chlamydomonas reinhardtii*, and the cyanobacterium *Synechococcus* (Fig. S2). In plants, PCD8 was predicted to be located in the chloroplast (Fig. S2; http://www.cbs.dtu.dk/services/ChloroP/). To confirm the subcellular localization of PCD8, we generated transgenic plants expressing the PCD8-GFP (green fluorescent protein) fusion protein driven by the CaMV 35*S* promoter. Results showed that the fusion protein locates in the chloroplast (Fig. 2f). Subsequent immunoblot analysis demonstrated that PCD8 is mainly localized in the thylakoid membrane (Fig. 2g). To investigate the effect of light on PCD8 expression, we analyzed the levels of *PCD8* transcript and protein in 4-d-old etiolated seedlings upon transition to light. Both transcript and protein levels of PCD8 increased after light exposure (Fig. S3a,b).

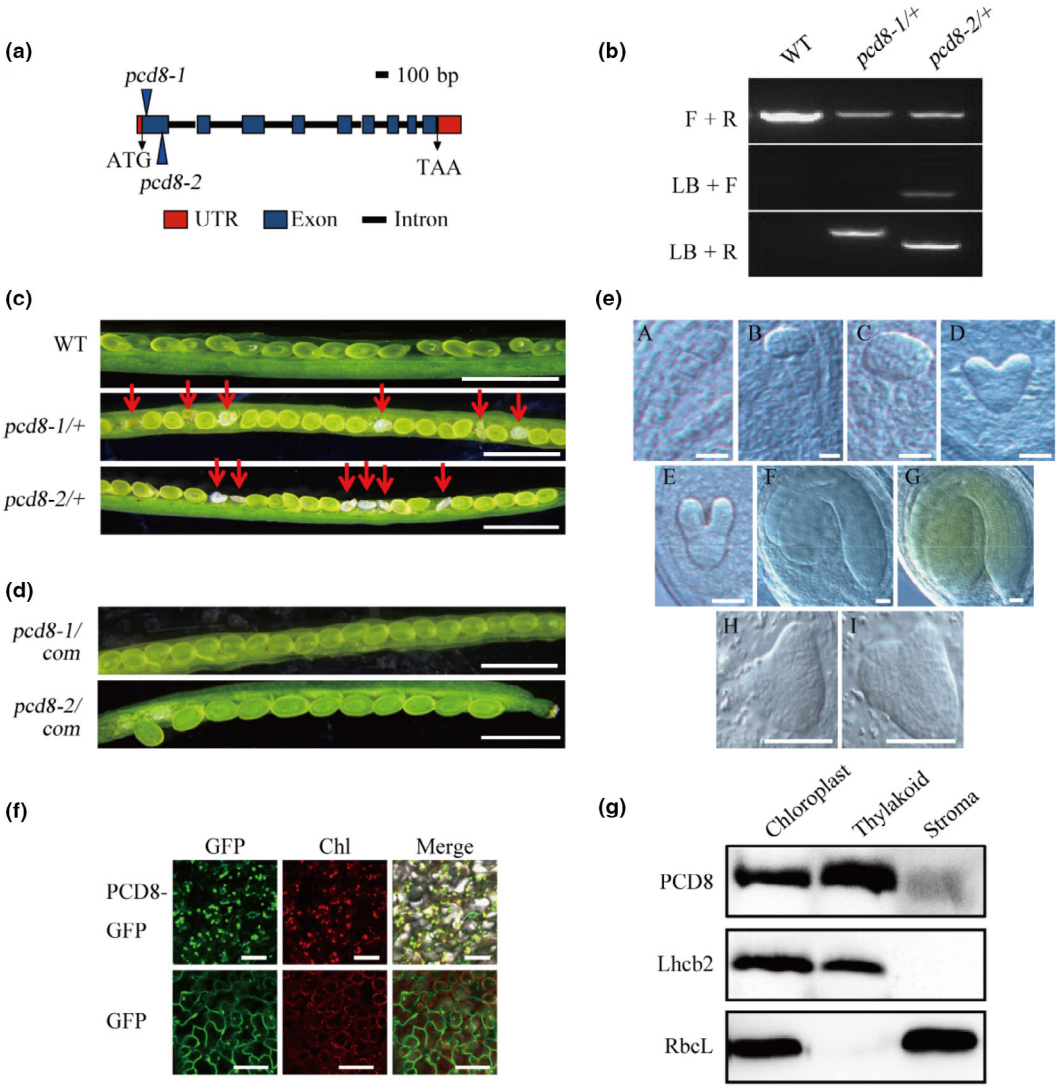

Fig. 2 PCD8 localizes to chloroplast thylakoid membranes and knocking-out *PCD8* gene causes embryo lethality in Arabidopsis. (a) Schematic representation of the *PCD8* locus and location of the T-DNA insertions (indicated by triangles). Exons are represented as boxes; start and stop codons are indicated. (b) Identification of heterozygous T-DNA insertions in *pcd8-1* and *pcd8-2* mutants by PCR using genomic DNA as a template. Primer combinations are indicated at the left. (c) Siliques from the Wild-type (WT) and heterozygous *pcd8-1*/+ and *pcd8-2*/+ plants observed with a stereomicroscope. Aborted seeds (suggesting embryo lethality) are marked by red arrows. Bars, 1 mm. (d) Siliques from *pcd8-1*/+ and *pcd8-2*/+ transgenic plants that express *PCD8* from its native promoter and 3′ UTR observed with a stereomicroscope. Bars, 1 mm. (e) Embryo phenotype of *pcd8-1*/+ and *pcd8-2*/+ mutants. WT embryos at the eight-cell stage (A), early globular stage (B), late globular stage (C), heart stage (D), torpedo stage (E), cotyledon stage (F), and mature embryo stage (G) are shown. Mutant embryos in aborted seeds from *pcd8-1*/+ (H) and *pcd82*/+ (I) are arrested at the heart stage. Bars, 20 μm. (f) Analysis of subcellular localization of the PCD8 protein by confocal laser-scanning microscopy. The PCD8-GFP fusion protein accumulates in the chloroplast. GFP, control line expressing an unfused GFP; Chl, chlorophyll fluorescence. Bars, 200 μm. (g) The PCD8 protein mainly localizes to the thylakoid membrane. Intact chloroplasts were isolated from 4-wk-old WT plants and then separated into thylakoid membranes and stroma. Polyclonal antibodies raised against PCD8 were used for protein identification. Antibodies against the thylakoid membrane protein Lhcb2 and antibodies against the abundant stromal protein RbcL served as marker proteins.

PCD8 RNAi mutants undergo chloroplast rupture and cell death upon transition from darkness to light

Next, we wanted to characterize the cell death processes that occur in leaves of *PCD8* RNAi mutants in more detail. To this end, we first assessed the number of dead cells semiquantitatively by Trypan blue staining. As shown in Fig. 3a, the cell death phenotype was apparent in all three *PCD8* RNAi lines, but not in the WT. Second, measurement of cellular ion leakage indicated that RNAi-14 and RNAi-21 plants significantly exhibited higher ion leakage than WT and RNAi-6 plants (Fig. 3b). Third, we found lower survival rates of the mutants than the WT, when seedlings grew in the dark for 3–6 d and were subsequently exposed to light for 48 h (Fig. 3c). Fourth, staining with SYTOX, an extracellular DNA dye, also confirmed cell death occurrence in the *PCD8* RNAi mutants (Fig. 3d). Fifth, chloroplast integrity

and cell death were assessed via monitoring the distribution of GFP fluorescence in RNAi-21 line expressing either a chloroplast-localized GFP or a cytosolic GFP. The damaged cell membranes in leaves of dark-grown RNAi-21 seedlings could be observed after 1 h of light exposure (Fig. 3e). Cellular damage was more evident in 28-d-old RNAi-21 plants grown under SD (Fig. S4a). The loss of chloroplast integrity of RNAi-21 upon dark-to-light transition was evidenced by detection of the plastid-targeted GFP in the cytosol (in conjunction with chloroplast rupture; Figs 3f, S4b). However, at present, we cannot fully exclude the possibility that reduced import also contributes to GFP accumulation in the cytosol. Finally, the ultrastructure of the chloroplasts was examined. In dark, etiolated seedlings of WT and RNAi mutants show similar structure of etioplasts. After de-etiolation, we observed shrunken cells in the mutants and damaged chloroplasts with separated stroma lamellae, large plastoglobules, and disrupted outer envelope membranes (Fig. 3g). Taken together, these results indicate that PCD8 plays an important role in chloroplast development during photoperiodic growth of Arabidopsis seedlings.

Singlet oxygen accumulation in the mutants likely causes the PCD phenotype

Previous studies have reported the initiation of PCD related to a burst of ROS, which is primarily generated in the chloroplast (Vacca *et al.*, 2006; De Pinto *et al.*, 2012; Wang & Bayles, 2013). We, therefore, investigated the accumulation of ROS in 5-d-old or 28-d-old SD-grown plants. Although the levels of hydrogen peroxide (H_2O_2) and superoxide anion ($O_2^{\bullet-}$) were similar between mutants and WT leaves (Figs 4a,b, S5a,b), $^1O_2$ could only be detected in the mutants (Fig. 4c). These results were generally in agreement with the expression levels of ROS-responsive genes, in which the two H_2O_2 marker genes (*APX1* and *Ferritin*) were downregulated (Fig. 4d) while ROS-responsive genes (*ZAT12*, *CYC8*, and *GST*) and $^1O_2$ marker genes (*LIT30*, *BAP1*, and *Atpase*) were significantly upregulated in RNAi-14 and RNAi-21 lines, compared with WT (Fig. 4e,f).

$^1O_2$ is produced in the chloroplast under excessive light conditions (Gonzalez-Perez *et al.*, 2011) and responsible for photooxidative damage (Triantaphylides *et al.*, 2008). Since anthocyanins are induced by high light and inhibited by $^1O_2$ (Vanderauwera *et al.*, 2005; Xu *et al.*, 2017), we examined anthocyanin content in seedlings exposed to excessive light (1000 $\mu mol\, m^{-2}\, s^{-1}$). As expected, light stress resulted in bleaching of leaves (Fig. S6a), and significantly reduced anthocyanin contents in RNAi-14 and RNAi-21 plants, compared with the WT (Fig. S6b). We also found that the maximum photochemical efficiency of photosystem II (F_v/F_m) was lower in RNAi-21 under SD conditions than in WT. By contrast, the F_v/F_m value of RNAi-21 was not significantly different from that of the WT after excess light treatment (Fig. S6c). Moreover, excess light lowered the differences in pigment content between the RNAi mutants and the WT (Fig. S6d). Taken together, these results suggest that knockdown of *PCD8* expression leads to specific accumulation of $^1O_2$ and thus triggered the cell death phenotype in leaves.

Several TBS intermediates and pathway enzymes overaccumulate in *PCD8* RNAi mutants under SD conditions

Based on previous reports that $^1O_2$ was derived from chlorophyll biosynthetic intermediates in the light (Kim & Apel, 2013b; Xu *et al.*, 2017), we determined the steady-state levels of chlorophylls and tetrapyrrole intermediates. When grown in CL, WT, and *PCD8* RNAi leaves contained similar contents of Chl*a*, Chl*b*, and carotenoids (Fig. S7a). However, WT seedlings accumulated a higher content of total chlorophyll than the mutants when 4-d-old etiolated seedlings were exposed to light for up to 48 h (Fig. S7b). By contrast, under SD conditions, RNAi-14 and RNAi-21 leaves contained *c.* 70% of the WT content of Chl*a*, Chl*b*, and carotenoids (Fig. 5a), but significantly higher levels of ALA and uroporphyrinogen III (Uro III; Fig. 5b–d). We found that chlorophyll intermediates, Proto IX, Mg-protoporphyrin IX (MgP), and Pchlide also accumulated higher in RNAi-21 than other RNAi lines and WT (Fig. 5e–i). These data suggest that excess accumulation of photosensitive intermediates, especially of Uro III, corresponds with the increase in $^1O_2$ content in *PCD8* RNAi mutants.

To investigate whether PCD8 regulates the levels of the above compounds at the translational level, we examined the expression levels of enzymes in TBS by immunoblot analysis with commercially available antibodies. Our results revealed that the steady-state levels of several TBS proteins were significantly higher in CL-grown *PCD8* RNAi mutants (Fig. 5j). By contrast, the transcript levels of genes encoding these enzymes were not or only slightly upregulated in *PCD8* RNAi mutants grown under CL (Fig. S8). These findings indicate that the increased contents of TBS proteins in *PCD8* RNAi mutants were not due to transcriptional regulation. In 28-d-old plants grown in SD, the transcription levels of many genes in the pathway were significantly downregulated in the *PCD8* RNAi mutants (Fig. S9a), compared with those in the WT, presumably due to the cellular damage caused by singlet oxygen release, while the protein accumulation was not dramatically reduced in comparison to their transcripts (Fig. S9b). Given such strong changes in enzyme levels under CL, we measured the level of Uro III in the WT and the RNAi mutants using 4-wk-old plants grown in soil under continuous dim light. The data showed that Uro III also overaccumulates in RNAi plants compared with the WT under CL (Fig. S10a). Under CL, the cotyledons of RNAi seedlings suffered from cell death (Fig. S10b), while the mature leaves showed no cell death (Fig. S10c). Taken together, these results suggest that PCD8 is a negative regulator for TBS proteins at a post-translational level.

The cell death phenotype of *PCD8* knockdown mutants depends on GUN4, GUN5, and EX1

GUN4 and GUN5 are proteins of the Mg-chelatase complex in the chlorophyll biosynthesis pathway. GUN4 interacts with GUN5 and stimulates Mg-chelatase activity (Larkin *et al.*, 2003). *GUN5* encodes the Mg-chelatase enzyme subunit (CHLH),

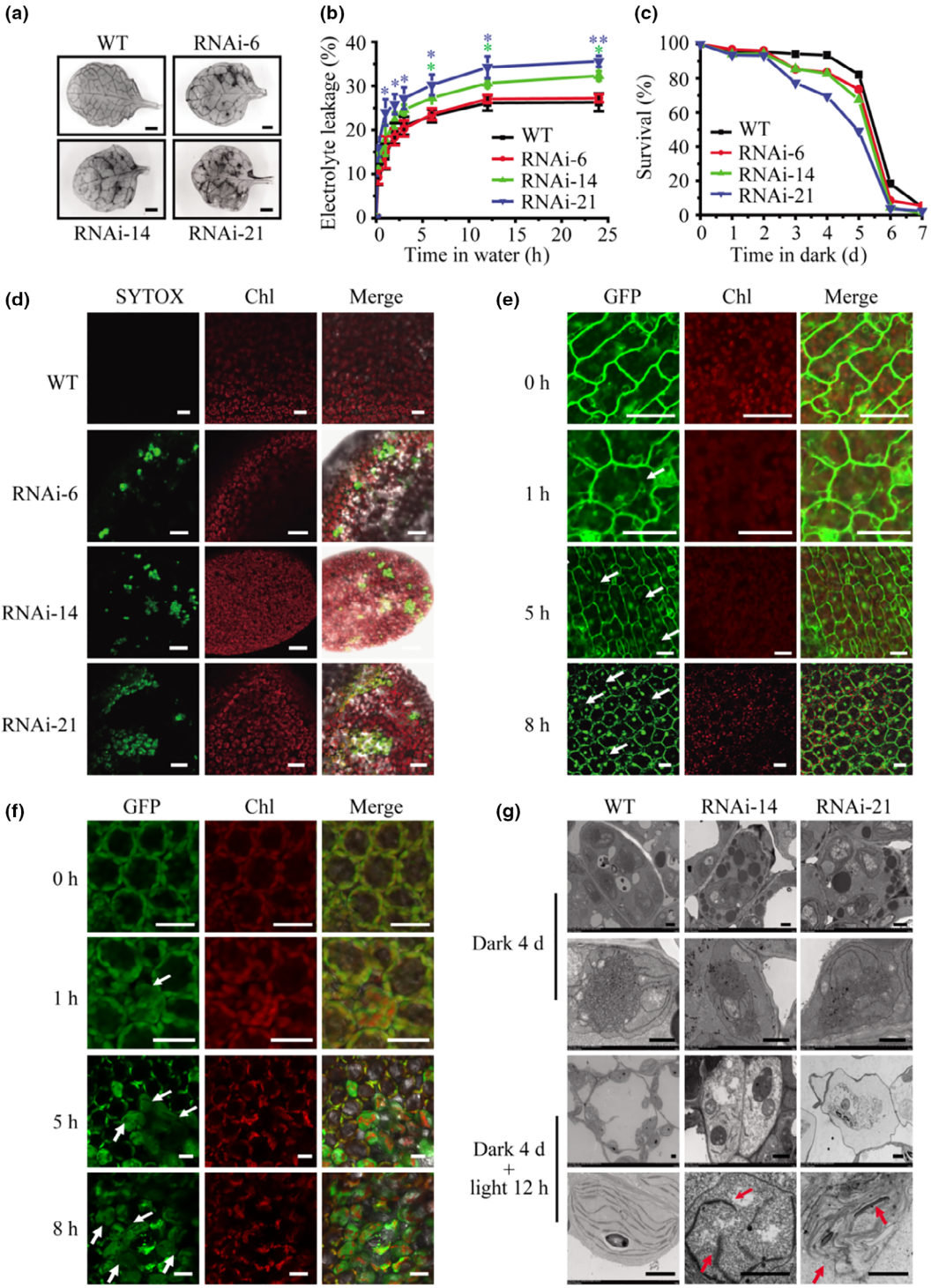

Fig. 3 Arabidopsis *PCD8* RNAi mutants suffer from cell death and chloroplast rupture. (a) Leaves of 28-d-old plants grown under short-day (SD) conditions were stained with Trypan blue. Dark sectors represent clusters of dead cells. Pictures were processed with ImageJ. (b) Ion leakage was measured at the indicated time points in 10-d-old seedlings grown under SD conditions. Fifteen seedlings per genotype were used for each measurement. Data are means ± standard deviation, $n = 3$ biological repetitions. Student's *t*-test: *, $P < 0.05$; **, $P < 0.01$. (c) Hundred seedlings of each line were grown in the dark for 0, 1, 2, 3, 4, 5, 6, or 7 d and then exposed to light for 48 h. Subsequently, the survival rates were determined. (d) Cotyledons of *PCD8* RNAi mutants undergo cell death, as revealed by SYTOX green staining. Seedlings were grown in the dark for 4 d and then exposed to light for 1 d. Chl, chlorophyll. Bars, 50 μm. (e, f) Representative confocal microscopy images of 4-d-old seedlings of *PCD8* RNAi mutants expressing a cytosolic GFP (e), or a plastid-targeted GFP (RBCS1B-GFP) (f). Seedlings were grown in the dark and exposed to light for 0, 1, 5, or 8 h. White arrows indicate damaged cell membranes (e) and cells with GFP that have leaked out of ruptured chloroplasts into the cytosol (f). Chl, chlorophyll. Bars, 20 μm. (g) RNAi mutants show cell death and chloroplast rupture. Representative transmission electron microscopy (TEM) images of cells and chloroplasts from seedlings grown in the dark for 4 d with or without subsequent exposure to the light for 12 h are shown. Bars, 1 μm. Red arrows indicate damaged chloroplasts.

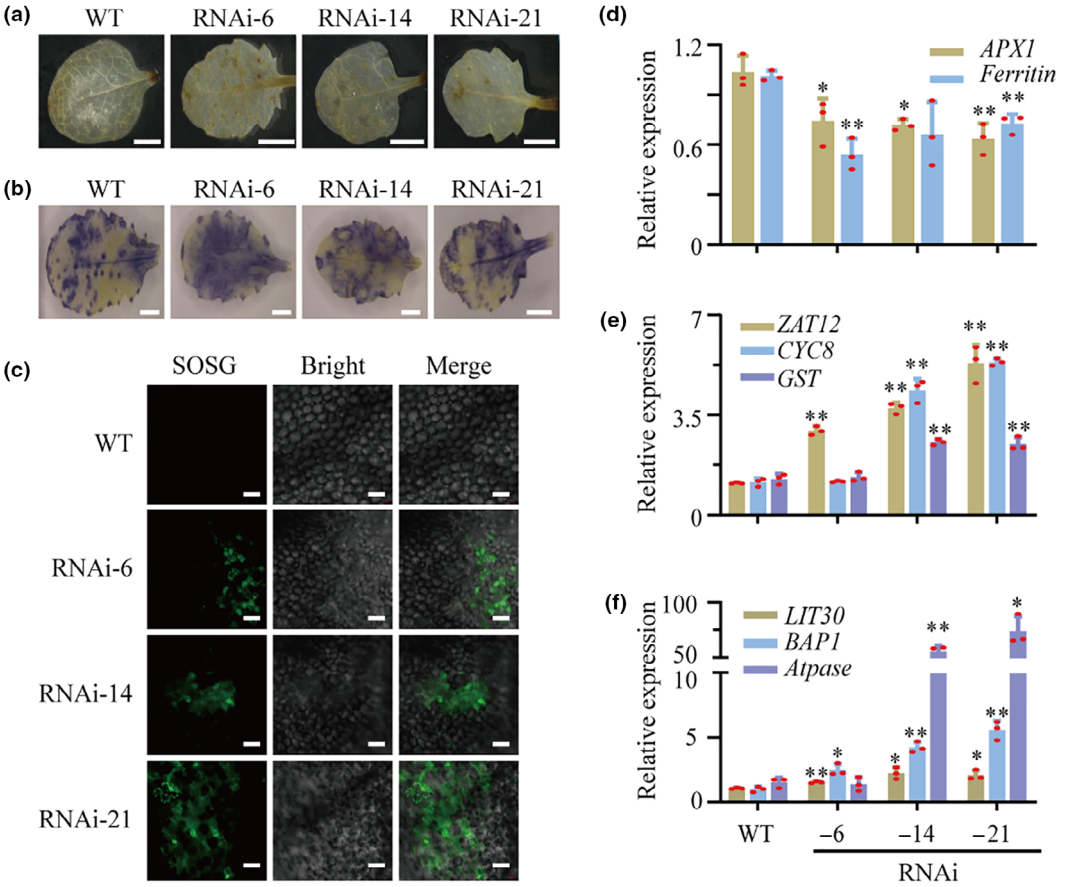

Fig. 4 Arabidopsis *PCD8* RNAi mutants accumulate $^1O_2$. (a) Diaminobenzidine staining to visualize H_2O_2 accumulation in leaves. Brown spots represent sites of H_2O_2 localization. Twenty-eight-day-old plants grown under short-day (SD) conditions were used. Bars, 2 mm. (b) Nitroblue tetrazolium staining to detect $O_2^{\bullet-}$ accumulation in leaves. Blue spots represent sites of $O_2^{\bullet-}$ localization. Twenty-eight-day-old plants grown under SD conditions were analyzed. Bars, 2 mm. (c) Singlet Oxygen Sensor Green (SOSG) staining to detect $^1O_2$ in seedling leaves. Green fluorescence represents $^1O_2$ accumulation. Five-day-old seedlings grown under SD conditions were analyzed. Bars, 20 μm. (d–f) Relative expression of H_2O_2 marker genes (d), general reactive oxygen species marker genes (e), and $^1O_2$ marker genes (f) in 4-wk-old RNAi mutants grown under SD conditions. The *EF1α* mRNA was used as internal control. Data are means ± standard deviation, $n = 3$ biological replicates. Student's *t*-test: *, $P < 0.05$; **, $P < 0.01$.

which binds the substrate Proto IX. It has been proposed that CHLH receives Proto from GUN4 (Mochizuki *et al.*, 2001; Adhikari *et al.*, 2011). The EX1 protein mediates $^1O_2$-triggered PCD in the *flu* mutant (Lee *et al.*, 2007; Kim *et al.*, 2012). To investigate whether GUN4, GUN5, and EX1 are involved in *PCD8* RNAi-21-mediated cell death, we made *21gun4*, *21gun5*, and *21ex1* double mutants (21 stands for *PCD8* RNAi-21) and examined their cell death phenotype under SD conditions. Interestingly, the phenotype of RNAi-21 was strongly suppressed by *gun4*, *gun5*, and *21ex1*, only showing few necrosis spots on old leaves (Fig. S11a). Pigment content analysis showed that introduction of *ex1* restored pigment accumulation of RNAi-21 to that of the WT, whereas *21gun4* and *21gun5* had similar pigment levels to *gun4* and *gun5*, which are significantly lower than those of the WT (Fig. S11b). In addition, an increased ion leakage due to the cell death was apparent in RNAi-21, while other mutants had no significant difference from the WT (Fig. S11c). Moreover, we found that *gun4* and *gun5* accumulated less Uro I, Uro III, and Pchlide than the WT, and the higher accumulation of Uro I, Uro III, and Pchlide in RNAi-21 was recovered by *gun4* and *gun5* to the WT level (Fig. S11d–f). Unexpectedly, the Uro I/III content in RNAi-21 was also significantly reduced by *ex1* (Fig. S11d,e), implying that EX1 may play a role in TBS. Consistent with these results, SOSG staining showed that *21ex1* also accumulates $^1O_2$, but to a much lower degree than the RNAi-21 line (Fig. S11g), suggesting that the $^1O_2$ signaling may not require mediation by EX1 in *PCD8* RNAi mutants. The fact that the double mutants do not show a cell death phenotype is most likely due to the reduced accumulation of tetrapyrrole intermediates in *gun4*, *gun5*, and *ex1*, which in turn supports the assumption that the excess accumulation of tetrapyrrole intermediates leads to cell death in *PCD8* RNAi mutants.

PCD8 interacts with the ClpC1 subunit of the Clp protease and several TBS enzymes

To identify interaction partners of PCD8, we extracted total proteins from the transgenic plants expressing PCD8-GFP and

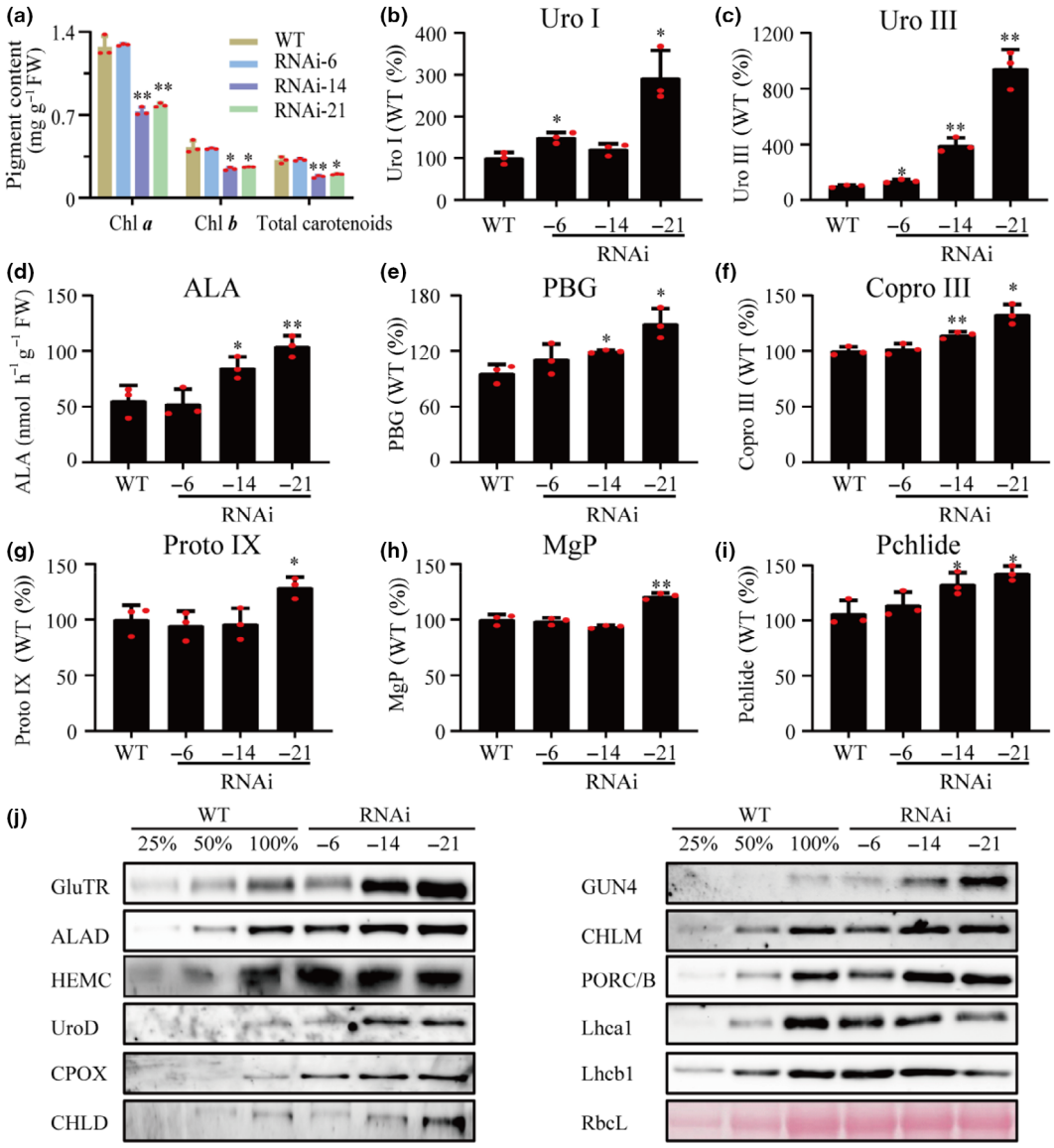

Fig. 5 PCD8 negatively regulates accumulation of several enzymes in the chlorophyll biosynthesis pathway in Arabidopsis. (a) Chl*a*, Chl*b*, and total carotenoids contents in 28-d-old plants grown under short-day (SD) conditions. $n = 3$ biological replicates. Student's *t*-test: *, $P < 0.05$; **, $P < 0.01$. (b–h) Quantification of Uro I (b), Uro III (c), aminolevulinic acid (ALA) synthesis rate (d), PBG (e), Copro III (f), Proto IX (g), and MgP (h) in plants grown under SD conditions for 18 d. (i) Determination of Pchlide in 4-d-old etiolated seedlings. Data are means of three independent biological replicates. Error bars indicate standard deviation. Student's *t*-test: *, $P < 0.05$; **, $P < 0.01$. (j) Steady-state levels of proteins involved in chlorophyll biosynthesis in 18-d-old seedlings grown under CL (low light: 30 μmol photons m^{-2} s^{-1}) conditions. Protein abundance was quantified by immunoblotting using the indicated antibodies. RbcL stained with Ponceau S served as loading control.

immunoprecipitated PCD8 complexes with the GFP antibody. Mass spectrometry analysis of the immunoprecipitates revealed that a number of chloroplast proteins including subunits of Clp protease (ClpC1, ClpP4, ClpP5, ClpP6, and ClpR4), and the TBS enzymes (porphobilinogen deaminase: HEMC, magnesium-chelatase subunit D: CHLD, protochlorophyllide reductase C: PORC, glutamyl-tRNA reductase-binding protein: GluTRBP, uroporphyrinogen decarboxylase: UroD, coproporphyrinogen III oxidase: CPOX, magnesium-chelatase subunit H: CHLH, and magnesium protoporphyrin IX methyltransferase: CHLM) were identified as PCD8-associated proteins (Table S2). We performed BiFC assays to confirm the mass spectrometry result. ClpC1, HEMC, CHLD, and PORC all interacted with PCD8, whereas HSP21 did not (used as a negative control; Fig. 6a). Likewise, split-luciferase (LUC) complementation assays indicated that LUC activity was strongly observed when PCD8 were co-expressed with ClpC1, HEMC, CHLD, or PORC, whereas no signal was determined in the negative controls (Fig. 6b). Additionally, pull-down assays demonstrated that PCD8 directly interacted with ClpC1, HEMC, and PORC (Fig. 6c–e). Interestingly, we found that the steady-state levels of the enzymes of the chlorophyll biosynthesis pathway were substantially increased in *clpC1* (Fig. 6f), similar to the observed increases in the *PCD8* RNAi mutants.

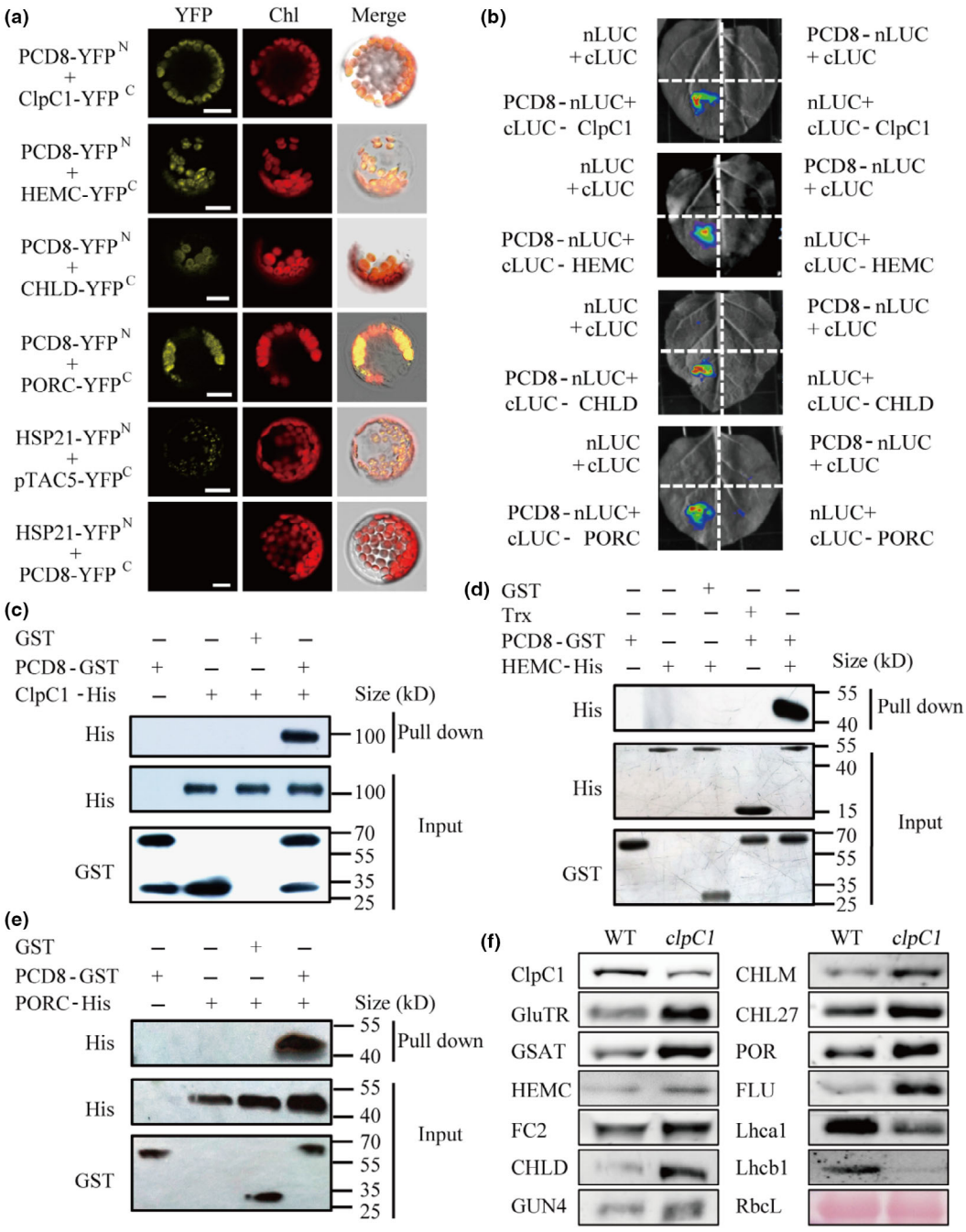

Fig. 6 PCD8 interacts with the ClpC1, HEMC, CHLD, and PORC proteins in Arabidopsis. (a) Interaction of PCD8 with ClpC1, HEMC, CHLD, and PORC in bimolecular fluorescence complementation assays. YFP fluorescence was observed when PCD8-YFP^N was co-expressed with ClpC1-YFP^C, HEMC-YFP^C, CHLD-YFP^C, or PORC-YFP^C in *Arabidopsis* protoplast. HSP21-YFP^N co-expressed with pTAC5-YFP^C or PCD8-YFP^C served as controls for specificity. Chl, chlorophyll. Bars, 10 μm. (b) Luciferase (LUC) complementation imaging (LCI) assays verifying that PCD8 interacts with ClpC1, HEMC, CHLD, and PORC in *Nicotiana benthamiana* leaves. Only co-transformations of PCD8 with ClpC1, HEMC, CHLD, or PORC yield fluorescence signals. (c–e) Pull-down assays show that PCD8 interacts with ClpC1, HEMC, and PORC *in vitro*. An anti-His antibody was used for pull-down. Input samples were analyzed by immunoblotting using anti-His and anti-GST antibodies. (f) Immunoblot analysis of indicated protein levels in the *clpC1* mutant grown under CL for 2 wk. The RbcL stained with Ponceau S is shown as control for equal loading.

We next produced double mutants of *clpC1* and the RNAi-21 line (subsequently referred to as *21clpC1*). Results showed that the phenotype of *21clpC1* was similar to that of *clpC1*, which displayed pale green leaves without necrotic spots (Figs 7a, S12), suggesting that *PCD8* acts upstream of *ClpC1*. Likewise, the contents of Uro I and Uro III in *21clpC1* were similar to that in *clpC1* and, thus, comparable to the WT (Fig. 7b). Consistently, immunoblot analysis showed that TBS proteins were substantially increased in *21clpC1* and accumulated even more than in *clpc1* (Fig. 7c). Taken together, our results suggest that PCD8

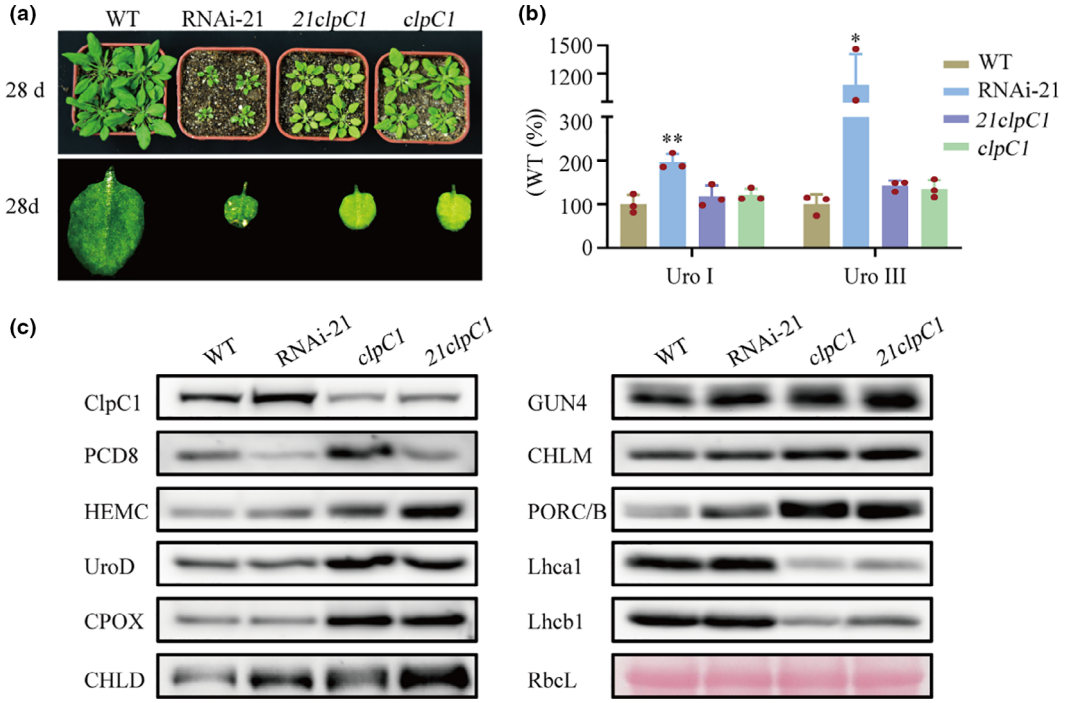

Fig. 7 Function of PCD8 depends on ClpC1 in Arabidopsis. (a) Phenotype of *21clpc1* double mutants grown under short-day (SD) conditions for 28 d. (b) Levels of Uro I and Uro III in plants grown under SD for 28 d. Data are means of three independent biological replicates. Error bars indicate standard deviation. $n = 3$ biological replicates. Student's *t*-test: *, $P < 0.05$; **, $P < 0.01$. (c) Immunoblot analysis of selected proteins related to chlorophyll biosynthesis in the *21clpC1* double mutant compared with the single mutants and the wild-type (WT). Plants were grown under CL for 18 d. The RbcL stained with Ponceau S is shown as control for equal loading.

contribute to the content of several TBS enzymes and, thus, impacts the flux of TBS. PCD8 is proposed to dedicate these TBS proteins to proteolysis by specifically recruiting them to the ClpC1 subunit of Clp protease.

Discussion

It has been reported that lack of TBS proteins encoded by a single gene causes embryo lethality or arrest of seedling growth. For example, *hemb1* (mutant of *HEMB1* gene encoding 5-aminolevulinic acid dehydratase (ALAD)) is embryo lethal at the globular stage (Tang *et al.*, 2012); soil grown *hemc* (mutant of *HEMC* gene encoding porphobilinogen deaminase) seedlings exhibit albino cotyledons and no true leaves (Huang *et al.*, 2017). In the present study, we identified a previously unknown chloroplast protein, PCD8. A *PCD8* null mutation leads to embryo lethality (Fig. 2), while a *PCD8* knockdown causes the leaf cell death phenotype due to overaccumulation of several tetrapyrrole intermediates and, subsequently, of $^1O_2$ during the dark-to-light transition (Figs 1, 4, 5). Interestingly, PCD8 directly interacts with several TBS enzymes (Fig. 6; Table. S2), suggesting a possible impact of PCD8 on the metabolic flux in the TBS pathway. Because free chlorophyll intermediates are phototoxic, their accumulation in the cell must be prevented. For this reason, chlorophyll biosynthesis is tightly regulated in response to endogenous stimuli and environmental cues (Mochizuki *et al.*, 2010; Brzezowski *et al.*, 2015). It has also been reported that downregulated expression of UroD in tobacco and maize leads to a necrotic phenotype due to the accumulation of Uro III (Mock & Grimm, 1997; Hu *et al.*, 1998). Similar light-dependent necrotic phenotypes and the accumulation of Uro I have been observed in a barley mutant, in which the Uro III synthase gene (*Uros*) was suppressed by antisense RNA expression (Ayliffe *et al.*, 2009). In this study, the elevated ALA synthesis capacity that represents the rate-limiting step of TBS (Fig. 5d), may lead to the uncontrolled accumulation of Uro I/III and possibly other intermediates in the *PCD8* RNAi lines (Fig. 5b,c), and ultimately to a $^1O_2$ burst and cell death under our growth conditions. Whether PCD8 directly participates in regulating ALA synthesis or TBS needs to be addressed in future studies. Interestingly, the $^1O_2$ signal in *PCD8* RNAi mutants is EX1-independent (Fig. S11). It, therefore, will be interesting to determine the site(s) of $^1O_2$ release and investigate the possible involvement of other components of $^1O_2$ signaling in the *PCD8* RNAi mutants.

Besides TBS enzymes, our results also show physical interaction of PCD8 with the Clp protease subunit ClpC1 (Fig. 6a–e, Table S2). The Clp protease is essential to eliminate unwanted proteins in plastids (Rodriguez-Concepcion *et al.*, 2019). The ClpC1 chaperone was reported to play an important role in the regulation of chlorophyll biosynthesis by directing GluTR and chlorophyllide *a* oxygenase to proteolysis (Nakagawara *et al.*, 2007; Apitz *et al.*, 2016). Our genetic results showed that *clpC1* suppresses the necrotic phenotype of RNAi-21, and consistent with this finding, the *21clpC1* double mutant had very similar Uro I/III contents as *clpC1* (Fig. 7a,b). In addition, several TBS enzymes overaccumulated in the *PCD8* RNAi mutants, *clpC1*, and 21*clpC1* mutants

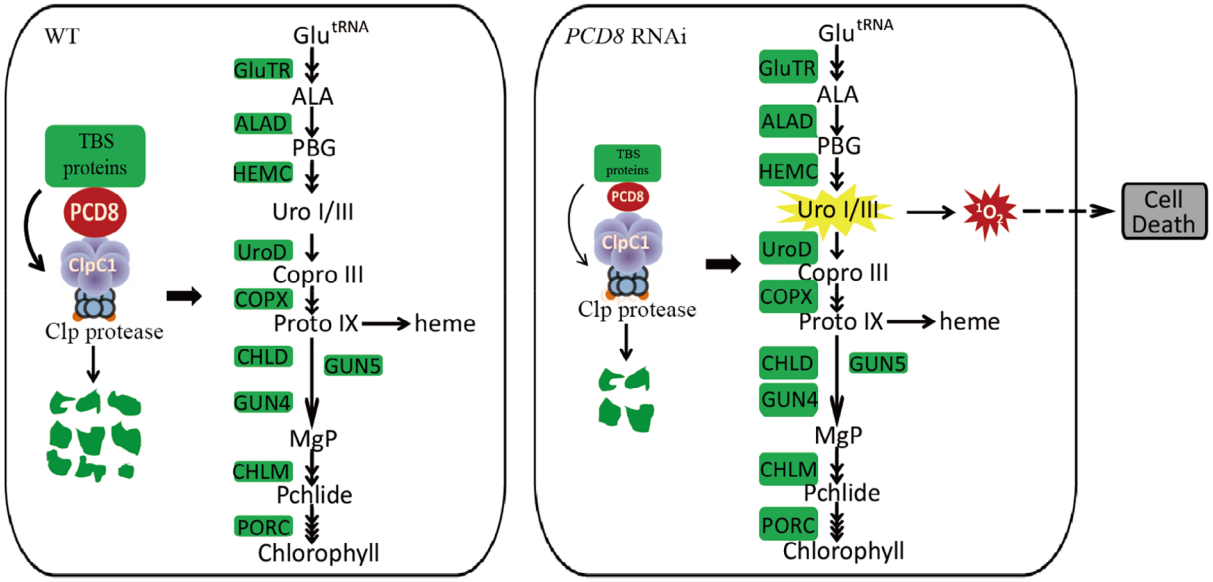

Fig. 8 Schematic model of PCD8 function in chlorophyll biosynthesis in Arabidopsis. (a) In the wild-type (WT), the Clp protease complex recruited by PCD8 controls the turnover of tetrapyrrole biosynthesis (TBS) enzymes to maintain steady-state levels of tetrapyrroles. (b) In *PCD8* RNAi mutants, TBS enzymes and tetrapyrrole intermediates are increased, and the overaccumulating tetrapyrrole intermediates, especially Uro III, generate a burst of $^1O_2$ upon light exposure, thus causing programmed cell death (PCD). The thick curved arrow represents that more TBS proteins are degraded by Clp protease, while the thin curved arrow represents that less TBS proteins are degraded by Clp protease.

(Figs 5j, 6f, 7c). We, therefore, propose that PCD8 acts upstream of ClpC1 and promotes the degradation of TBS protein by the Clp protease. This model also explains why inactivation of PCD8 or ClpC1 leads to excessive accumulation of TBS proteins.

Our studies demonstrate that PCD8 affects accumulation of TBS proteins at a post-translational level (Fig. S8). It is suggested that multiple post-translational ways are essential for the tight and rapid regulation of the key step in the chlorophyll biosynthesis pathway to adapt the supply of chlorophyll and heme to changing environmental conditions (Stenbaek & Jensen, 2010; Czarnecki & Grimm, 2012). These post-translational control mechanisms include assembly of heteromultimeric protein complexes and redox control of enzyme activity (Kauss *et al.*, 2012; Richter *et al.*, 2013). Formation of multienzyme complexes *in vivo* is an efficient strategy to facilitate metabolic channeling and control of chlorophyll biosynthesis in locally restricted subcellular compartments (Brzezowski *et al.*, 2015). Some specific signaling motifs in the protein structure (named degrons) of substrates, such as post-translational modification (phosphorylation, acetylation, etc.) are recognized by a specific protein (auxiliary factor, assistant protein, and co-regulator) to mediate the delivery of substrate protein to Clp protease for degradation (Rodriguez-Concepcion *et al.*, 2019). Therefore, it is possible that PCD8 mutually interacts with Clp and TBS enzymes, thus facilitating the precise regulation of the TBS pathway.

Based on the physiological and molecular functions of PCD8 discovered in this study, we propose a working model of PCD8 (Fig. 8). In the WT, PCD8 interacts with ClpC1 and recruits TBS enzymes to Clp protease, and thus maintains the homeostasis of TBS by controlling the degradation of TBS enzymes through Clp protease. In *PCD8* RNAi mutants, several TBS enzymes overaccumulate, resulting in uncontrolled increase in tetrapyrrole intermediates, including Uro I and Uro III, and triggering a burst of $^1O_2$ during the transition from the dark to light. Our working model raises the intriguing question, why accumulation of TBS enzymes in the absence of PCD8, but not of ClpC1, causes build-up of the phototoxic chlorophyll precursors. The ClpC1 subunits of the Clp protease act as chaperone that unfolds substrate proteins (Rodriguez-Concepcion *et al.*, 2019). The Clp protease has a broad range of targets in the plastid. In addition, ClpC1 is also associated with the chloroplast protein import apparatus, and leaf iron homeostasis (Kovacheva *et al.*, 2007; Wu *et al.*, 2010). Consequently, inactivation of ClpC1 has a more general impact on many processes in plastid, including gene expression, proteins, metabolism, and biogenesis. This assumption is consistent with the yellow leaf phenotype and the lowered photosynthetic activity of the *clpC1* mutant (Sjögren *et al.*, 2004). However, based on the genetic and physiological data presented here, we propose that PCD8 acts specifically on a few target proteins in the TBS pathway dedicated for degradation. To fully elucidate the molecular mechanisms underlying PCD8-mediated biological processes, it will be important to identify the key factors that are primarily regulated by PCD8 in future investigations. In summary, our work reported here identifies a new factor involved in protection from PCD and provides new insights into the molecular mechanism fine-tuning the TBS pathway in plants.

Acknowledgements

WZ was supported by the Innovation Program of the Chinese Academy of Agricultural Sciences, the Elite Youth Program of

the Chinese Academy of Agricultural Science, and by a grant from the National Natural Science Foundation (31570234). We are grateful to Dr Chanhong Kim (Shanghai Center for Plant Stress Biology and CAS Center for Excellence in Molecular Plant Sciences) for providing *ex1* mutant, and Dr Robert Larkin (Michigan State University) for providing *gun4* and *gun5* mutants.

Competing interests

None declared.

Author contributions

WZ and RG conceived and designed the research. RG performed most of the experiments. XP conducted Western blot of TBS proteins. XL and SS performed the hybridization. RG, XP, BH and BG conducted the pigment measurements. All authors contributed to data evaluation and interpretation. WZ, RG, RB, BG and JH wrote the manuscript. All authors read and approved the final manuscript.

ORCID

Ralph Bock https://orcid.org/0000-0001-7502-6940
Rudan Geng https://orcid.org/0000-0002-4602-8178
Bernhard Grimm https://orcid.org/0000-0002-9730-1074
Boris Hedtke https://orcid.org/0000-0002-1170-1246
Jirong Huang https://orcid.org/0000-0002-4032-4566
Xia Li https://orcid.org/0000-0001-9933-6679
Xiaoqing Pang https://orcid.org/0000-0002-9266-3738
Wenbin Zhou https://orcid.org/0000-0001-5911-1686

Data availability

A complete version of Methods S1 and the data that support the findings of this study are available in the Supporting Information.

References

Adhikari ND, Froehlich JE, Strand DD, Buck SM, Kramer DM, Larkin RM. 2011. GUN4-porphyrin complexes bind the ChlH/GUN5 subunit of Mg-Chelatase and promote chlorophyll biosynthesis in Arabidopsis. *Plant Cell* **23**: 1449–1467.

Albus CA, Ruf S, Schottler MA, Lein W, Kehr J, Bock R. 2010. Y3IP1, a nucleus-encoded thylakoid protein, cooperates with the plastid-encoded Ycf3 protein in photosystem I assembly of tobacco and *Arabidopsis*. *Plant Cell* **22**: 2838–2855.

Apitz J, Nishimura K, Schmied J, Wolf A, Hedtke B, van Wijk KJ, Grimm B. 2016. Posttranslational control of ALA synthesis includes GluTR degradation by Clp protease and stabilization by GluTR-binding protein. *Plant Physiology* **170**: 2040–2051.

Ayliffe MA, Agostino A, Clarke BC, Furbank R, von Caemmerer S, Pryor AJ. 2009. Suppression of the barley uroporphyrinogen III synthase gene by a *Ds* activation tagging element generates developmental photosensitivity. *Plant Cell* **21**: 814–831.

Brzezowski P, Richter AS, Grimm B. 2015. Regulation and function of tetrapyrrole biosynthesis in plants and algae. *Biochimica et Biophysica Acta* **1847**: 968–985.

Clough SJ, Bent AF. 1998. Floral dip: a simplified method for Agrobacterium-mediated transformation of *Arabidopsis thaliana*. *The Plant Journal* **16**: 735–743.

Czarnecki O, Grimm B. 2012. Post-translational control of tetrapyrrole biosynthesis in plants, algae, and cyanobacteria. *Journal of Experimental Botany* **63**: 1675–1687.

D'Alessandro S, Beaugelin I, Havaux M. 2020. Tanned or sunburned: how excessive light triggers plant cell death. *Molecular Plant* **2**: 1545–1555.

D'Alessandro S, Ksas B, Havaux M. 2018. Decoding β-cyclocitral-mediated retrograde signaling reveals the role of a detoxification response in plant tolerance to photooxidative stress. *Plant Cell* **30**: 2495–2511.

De Pinto MC, Locato V, De Gara L. 2012. Redox regulation in plant programmed cell death. *Plant, Cell & Environment* **35**: 234–244.

Demmig-Adams B, Adams WW III. 2000. Harvesting sunlight safely. *Nature* **403**: 373–374.

Dogra V, Li MY, Singh S, Li MP, Kim C. 2019. Oxidative post-translational modification of EXECUTER1 is required for singlet oxygen sensing in plastids. *Nature Communications* **10**: 2834.

Dogra V, Singh RM, Li M, Li M, Singh S, Kim C. 2022. EXECUTER2 modulates the EXECUTER1 signalosome through its singlet oxygen-dependent oxidation. *Molecular Plant* **15**: 438–453.

Gonzalez-Perez S, Gutierrez J, Garcia-Garcia F, Osuna D, Dopazo J, Lorenzo O, Revuelta JL, Arellano JB. 2011. Early transcriptional defense responses in *Arabidopsis* cell suspension culture under high-light conditions. *Plant Physiology* **156**: 1439–1456.

Hilson P, Allemeersch J, Altmann T, Aubourg S, Avon A, Beynon J, Bhalerao RP, Bitton F, Caboche M, Cannoot B *et al.* 2004. Versatile gene-specific sequence tags for *Arabidopsis* functional genomics: transcript profiling and reverse genetics applications. *Genome Research* **14**: 2176–2189.

Hu G, Yalpani N, Briggs SP, Johal GS. 1998. A porphyrin pathway impairment is responsible for the phenotype of a dominant disease lesion mimic mutant of maize. *Plant Cell* **10**: 1095–1105.

Huang C, Yu QB, Li ZR, Ye LS, Xu L, Yang ZN. 2017. Porphobilinogen deaminase HEMC interacts with the PPR-protein AtECB2 for chloroplast RNA editing. *The Plant Journal* **92**: 546–556.

Huang M, Slewinski TL, Baker RF, Janick-Buckner D, Buckner B, Johal GS, Braun DM. 2009. Camouflage patterning in maize leaves results from a defect in porphobilinogen deaminase. *Molecular Plant* **2**: 773–789.

Huysmans M, Lema AS, Coll NS, Nowack MK. 2017. Dying two deaths – programmed cell death regulation in development and disease. *Current Opinion in Plant Biology* **35**: 37–44.

Inaba T, Ito-Inaba Y. 2010. Versatile roles of plastids in plant growth and development. *Plant Cell Physiology* **51**: 1847–1853.

Ishikawa A, Okamoto H, Iwasaki Y, Asahi T. 2001. A deficiency of coproporphyrinogen III oxidase causes lesion formation in *Arabidopsis*. *The Plant Journal* **27**: 89–99.

Izumi M, Ishida H, Nakamura S, Hidema J. 2017. Entire photodamaged chloroplasts are transported to the central vacuole by autophagy. *Plant Cell* **29**: 377–394.

Jarvis P, Lopez-Juez E. 2013. Biogenesis and homeostasis of chloroplasts and other plastids. *Nature Reviews Molecular Cell Biology* **14**: 787–802.

Kauss D, Bischof S, Steiner S, Apel K, Meskauskiene R. 2012. FLU, a negative feedback regulator of tetrapyrrole biosynthesis, is physically linked to the final steps of the Mg^{++}-branch of this pathway. *FEBS Letters* **586**: 211–216.

Kim C, Apel K. 2013b. Singlet oxygen-mediated signaling in plants: moving from *flu* to wild type reveals an increasing complexity. *Photosynthesis Research* **116**: 455–464.

Kim C, Lee KP, Baruah A, Nater M, Gobel C, Feussner I, Apel K. 2009. $^1O_2$-mediated retrograde signaling during late embryogenesis predetermines plastid differentiation in seedlings by recruiting abscisic acid. *Proceedings of the National Academy of Sciences, USA* **106**: 9920–9924.

Kim C, Meskauskiene R, Zhang S, Lee KP, Lakshmanan Ashok M, Blajecka K, Herrfurth C, Feussner I, Apel K. 2012. Chloroplasts of *Arabidopsis* are the source and a primary target of a plant-specific programmed cell death signaling pathway. *Plant Cell* **24**: 3026–3039.

Kovacheva S, Bédard J, Wardle A, Patel R, Jarvis P. 2007. Further *in vivo* studies on the role of the molecular chaperone, Hsp93, in plastid protein import. *The Plant Journal* **50**: 364–379.

Kruse E, Mock HP, Grimm B. 1995. Reduction of coproporphyrinogen oxidase level by antisense RNA synthesis leads to deregulated gene expression of plastid proteins and affects the oxidative defense system. *EMBO Journal* **14**: 3712–3720.

Laloi C, Stachowiak M, Pers-Kamczyc E, Warzych E, Murgia I, Apel K. 2007. Cross-talk between singlet oxygen- and hydrogen peroxide-dependent signaling of stress responses in *Arabidopsis thaliana*. *Proceedings of the National Academy of Sciences, USA* **104**: 672–677.

Larkin RM, Alonso JM, Ecker JR, Chory J. 2003. GUN4, a regulator of chlorophyll synthesis and intracellular signaling. *Science* **299**: 902–906.

Lee KP, Kim C, Landgraf F, Apel K. 2007. EXECUTER1- and EXECUTER2-dependent transfer of stress-related signals from the plastid to the nucleus of *Arabidopsis thaliana*. *Proceedings of the National Academy of Sciences, USA* **104**: 10270–10275.

Lichtenthaler HK. 1987. Chlorophylls and carotenoids: pigments of photosynthetic biomembranes. *Methods in Enzymology* **148**: 350–382.

Lv R, Li Z, Li M, Dogra V, Lv S, Liu R, Lee KP, Kim C. 2019. Uncoupled expression of nuclear and plastid photosynthesis-associated genes contributes to cell death in a lesion mimic mutant. *Plant Cell* **31**: 210–230.

Meskauskiene R, Nater M, Goslings D, Kessler F, op den Camp R, Apel K. 2001. FLU: a negative regulator of chlorophyll biosynthesis in *Arabidopsis thaliana*. *Proceedings of the National Academy of Sciences, USA* **98**: 12826–12831.

Miernyk JA, Thelen JJ. 2008. Biochemical approaches for discovering protein-protein interactions. *The Plant Journal* **53**: 597–609.

Mochizuki N, Brusslan JA, Larkin R, Nagatani A, Chory J. 2001. *Arabidopsis genomes uncoupled 5* (*GUN5*) mutant reveals the involvement of Mg-chelatase H subunit in plastid-to-nucleus signal transduction. *Proceedings of the National Academy of Sciences, USA* **98**: 2053–2058.

Mochizuki N, Tanaka R, Grimm B, Masuda T, Moulin M, Smith AG, Tanaka A, Terry MJ. 2010. The cell biology of tetrapyrroles: a life and death struggle. *Trends in Plant Science* **15**: 488–498.

Mock HP, Grimm B. 1997. Reduction of uroporphyrinogen decarboxylase by antisense RNA expression affects activities of other enzymes involved in tetrapyrrole biosynthesis and leads to light-dependent necrosis. *Plant Physiology* **113**: 1101–1112.

Mock HP, Heller W, Molinai A, Neubohn B, Sandermann H Jr, Grimm B. 1999. Expression of uroporphyrinogen decarboxylase or coproporphyrinogen oxidase antisense RNA in tobacco induces pathogen defense responses conferring increased resistance to tobacco mosaic virus. *Journal of Biological Chemistry* **274**: 4231–4238.

Nakagawara E, Sakuraba Y, Yamasato A, Tanaka R, Tanaka A. 2007. Clp protease controls chlorophyll *b* synthesis by regulating the level of chlorophyllide *a* oxygenase. *The Plant Journal* **49**: 800–809.

Neuhaus HE, Emes MJ. 2000. Nonphotosynthetic metabolism in plastids. *Annual Review of Plant Physiology and Plant Molecular Biology* **51**: 111–140.

Pennell RI, Lamb C. 1997. Programmed cell death in plants. *Plant Cell* **9**: 1157–1168.

Quesada V, Sarmiento-Manus R, Gonzalez-Bayon R, Hricova A, Ponce MR, Micol JL. 2013. PORPHOBILINOGEN DEAMINASE deficiency alters vegetative and reproductive development and causes lesions in *Arabidopsis*. *PLoS ONE* **8**: e53378.

Rabino I, Mancinelli AL. 1986. Light, temperature, and anthocyanin production. *Plant Physiology* **81**: 922–924.

Richter AS, Peter E, Rothbart M, Schlicke H, Toivola J, Rintamaki E, Grimm B. 2013. Posttranslational influence of NTRC on enzymes in tetrapyrrole synthesis. *Plant Physiology* **162**: 63–73.

Rodriguez-Concepcion M, D'Andrea L, Pulido P. 2019. Control of plastidial metabolism by the Clp protease complex. *Journal of Experimental Botany* **70**: 2049–2058.

Salvi D, Rolland N, Joyard J, Ferro M. 2008. Purification and proteomic analysis of chloroplasts and their sub-organellar compartments. *Methods in Molecular Biology* **432**: 19–36.

Shumbe L, Chevalier A, Legeret B, Taconnat L, Monnet F, Havaux M. 2016. Singlet oxygen-induced cell death in Arabidopsis under high-light stress is controlled by OXI1 kinase. *Plant Physiology* **170**: 1757–1771.

Sjögren LL, MacDonald TM, Sutinen S, Clarke AK. 2004. Inactivation of the *clpC1* gene encoding a chloroplast Hsp100 molecular chaperone causes growth retardation, leaf chlorosis, lower photosynthetic activity, and a specific reduction in photosystem content. *Plant Physiology* **136**: 4114–4126.

Stenbaek A, Jensen PE. 2010. Redox regulation of chlorophyll biosynthesis. *Phytochemistry* **71**: 853–859.

Tang W, Wang W, Chen D, Ji Q, Jing Y, Wang H, Lin R. 2012. Transposase-derived proteins FHY3/FAR1 interact with PHYTOCHROME-INTERACTING FACTOR1 to regulate chlorophyll biosynthesis by modulating *HEMB1* during deetiolation in *Arabidopsis*. *Plant Cell* **24**: 1984–2000.

Triantaphylides C, Krischke M, Hoeberichts FA, Ksas B, Gresser G, Havaux M, Van Breusegem F, Mueller MJ. 2008. Singlet oxygen is the major reactive oxygen species involved in photooxidative damage to plants. *Plant Physiology* **148**: 960–968.

Vacca RA, Valenti D, Bobba A, Merafina RS, Passarella S, Marra E. 2006. Cytochrome *c* is released in a reactive oxygen species-dependent manner and is degraded via caspase-like proteases in tobacco bright-yellow 2 cells en route to heat shock-induced cell death. *Plant Physiology* **141**: 208–219.

Van Aken O, Van Breusegem F. 2015. Licensed to kill: mitochondria, chloroplasts, and cell death. *Trends in Plant Science* **20**: 754–766.

Vanderauwera S, Zimmermann P, Rombauts S, Vandenabeele S, Langebartels C, Gruissem W, Inze D, Van Breusegem F. 2005. Genome-wide analysis of hydrogen peroxide-regulated gene expression in *Arabidopsis* reveals a high light-induced transcriptional cluster involved in anthocyanin biosynthesis. *Plant Physiology* **139**: 806–821.

Wang J, Bayles KW. 2013. Programmed cell death in plants: lessons from bacteria? *Trends in Plant Science* **18**: 133–139.

Wang L, Leister D, Guan L, Zheng Y, Schneider K, Lehmann M, Apel K, Kleine T. 2020. The *Arabidopsis* SAFEGUARD1 suppresses singlet oxygen-induced stress responses by protecting grana margins. *Proceedings of the National Academy of Sciences, USA* **117**: 6918–6927.

Wang P, Grimm B. 2021. Connecting chlorophyll metabolism with accumulation of the photosynthetic apparatus. *Trends in Plant Science* **26**: 484–495.

Woodson JD, Joens MS, Sinson AB, Gilkerson J, Salome PA, Weigel D, Fitzpatrick JA, Chory J. 2015. Ubiquitin facilitates a quality-control pathway that removes damaged chloroplasts. *Science* **350**: 450–454.

Wu H, Ji Y, Du J, Kong D, Liang H, Ling HQ. 2010. ClpC1, an ATP-dependent Clp protease in plastids, is involved in iron homeostasis in *Arabidopsis* leaves. *Annals of Botany* **105**: 823–833.

Xu Z, Mahmood K, Rothstein SJ. 2017. ROS induces anthocyanin production via late biosynthetic genes and anthocyanin deficiency confers the hypersensitivity to ROS-generating stresses in *Arabidopsis*. *Plant Cell Physiology* **58**: 1364–1377.

Yoo SD, Cho YH, Sheen J. 2007. *Arabidopsis* mesophyll protoplasts: a versatile cell system for transient gene expression analysis. *Nature Protocols* **2**: 1565–1572.

Zhong L, Zhou W, Wang H, Ding S, Lu Q, Wen X, Peng L, Zhang L, Lu C. 2013. Chloroplast small heat shock protein HSP21 interacts with plastid nucleoid protein pTAC5 and is essential for chloroplast development in *Arabidopsis* under heat stress. *Plant Cell* **25**: 2925–2943.

Supporting Information

Additional Supporting Information may be found online in the Supporting Information section at the end of the article.

Fig. S1 Dark-to-light transitions are required to reveal the cell death phenotype of Arabidopsis *PCD8* RNAi mutants.

Fig. S2 Alignment of the amino acid sequences of PCD8 from selected plant species.

Fig. S3 Expression pattern of PCD8 protein in Arabidopsis.

Fig. S4 Arabidopsis *PCD8* RNAi mutants suffer from cell death and chloroplast rupture in 28-d-old plants grown under SD conditions.

Fig. S5 Arabidopsis *PCD8* RNAi mutants do not accumulate excess H_2O_2 and $O_2^{\bullet -}$ in seedlings.

Fig. S6 Arabidopsis *PCD8* RNAi mutants show altered pigment and anthocyanin contents.

Fig. S7 Absence of significant differences in pigment contents between Arabidopsis PCD8 RNAi mutants and wild-type plants (WT) under CL.

Fig. S8 Chlorophyll biosynthesis genes are not or only slightly upregulated in the Arabidopsis *PCD8* RNAi mutants grown under CL.

Fig. S9 Accumulation of transcripts and proteins related to the chlorophyll biosynthesis pathway in Arabidopsis *PCD8* RNAi mutants grown under SD.

Fig. S10 Uro III content and phenotypes of wild-type (WT) and Arabidopsis *PCD8* RNAi mutants under CL.

Fig. S11 *gun4*, *gun5*, and *ex1* suppress the phenotype of the Arabidopsis *PCD8* RNAi-21 mutant.

Fig. S12 No cell death occurred in Arabidopsis *21clpC1* leaves.

Methods S1 Detailed Materials and Methods.

Table S1 Mutant plants used in this study.

Table S2 Summary of mass spectrometric identification of proteins that co-immunoprecipitated with PCD8 from three independent experiments (Exp-1 to Exp-3) in Arabidopsis.

Table S3 Primers used in this study.

Please note: Wiley is not responsible for the content or functionality of any Supporting Information supplied by the authors. Any queries (other than missing material) should be directed to the *New Phytologist* Central Office.